Integrated Space-Division Multiplexer for Application to Data Center Networks

Andrew Grieco, George Porter, and Yeshaiahu Fainman, *Fellow, IEEE*

***Abstract*—The prospect of creating integrated space-division multiplexing (SDM) on a chip, utilizing the orthogonal degrees of freedom of numerous guided spatial modes in a multimode waveguide, promises a substantial reduction in the cost, complexity, and scalability of networking systems by augmenting or replacing the commonly used approach of wavelength-division multiplexing (WDM). As a demonstration of the SDM approach, we introduce and experimentally characterize a periodically nanostructured resonant coupler integrated with a multimode waveguide that selectively transfers energy between arbitrary waveguide modes. Compared to alternative schemes, this device possesses advantages in terms of packing density, control of operating bandwidth, tunability to operate with numerous orthogonal spatial modes, and support of a large number of switching ports.**

***Index Terms*—Bragg gratings, multiplexing, integrated optics.**

I. Introduction

THE widespread adoption of 'cloud computing' has led to the construction of data center networks that support up to hundreds of thousands of servers that need to communicate internally with each other at high server-to-server, or bi-section, bandwidths orders of magnitude greater than their connections to end users. These networks must scale with rapid user demand increases while keeping cost and energy requirements low. Today, scaling a network fabric to such a large scale is a significant challenge. To better support data center traffic, several recent efforts have begun to examine the suitability of building hybrid networks [1]–[9], which include both electrical packet switches and reconfigurable optical circuit switches (OCS). To meet cost, scalability in size and number of switching ports count, as well as reduction in energy requirements, we envision new hybrid data center designs whose photonic component resides on a chip [9].

Initial deployments [1]–[3] have shown that the reconfiguration switching time of the photonic switch is critical to support rapidly-changing traffic patterns such as all-to-all and gather/scatter traffic patterns present in large-scale applications such as MapReduce and web search. Recently, a fast OCS switch called Microsecond Optical Research Datacenter Interconnect Architecture (MORDIA) has been constructed and demonstrated [6]–[8]. The MORDIA system is based on a wavelength-selective switch with switching speed on the order of ten microseconds. At this speed, it can support traffic at the Top-of-Rack switch [10].

It is evident that next generation Data Centers will greatly benefit from integrating the costly discrete components on a single chip. For example, MORDIA, the fast OCS hybrid network system for datacenters, could be integrated on the silicon on insulator (SOI) material platform by combining CMOS compatible monolithic integration (e.g., modulators, add/drops, filters, detectors, etc. [11]–[13]) with heterogeneously integrated III-V compound semiconductor laser sources on a wavelength-division multiplexing (WDM) grid [14]–[16]. However, it should be noted that such an integrated system would be costly and complex due to the need to integrate and control the laser sources, remove heat, and stabilize the system for operation in practical environments (e.g. temperature stabilization, monitoring the lasers and receivers on WDM grid, etc.). In this context it is worthwhile to consider space-division multiplexing (SDM) as an alternative to augment or replace WDM [17]–[19]. Rather than rely on multiple wavelengths, such an approach would employ the orthogonal spatial modes supported by a multimode waveguide, where each server can be assigned to transmit on a specific spatial mode excited from a drop port as shown in Fig. 1. Likewise, its receiver will be supplied by a spatial mode drop port. The servers will then be able to use inexpensive standard transceivers transmitting information on the same standard laser carrier, substantially reducing the cost of the whole system.

The concept of SDM, also known by the equivalent term mode-division multiplexing (MDM), has been known in the context of guided wave optics for decades [20]–[22]. The earliest experimental demonstrations occurred in optical fiber with the same underlying motivation as today, namely the desire to improve the transmission capacity of optical networks. In multimode fiber (MMF) this approach has proven to be unfeasible for a number of reasons, including: difficulty in selectively exciting the modes of a MMF, crosstalk caused by mode coupling due to bending or other perturbations of the MMF, and mode dispersion which severely limits the data rates that can be achieved given the typical fiber propagation length. The advent of integrated photonics has provided a platform free of the limitations that prohibit SDM in fiber systems. Specifically, the integrated photonic chip platform is stable and crosstalk resistant, and the propagation lengths involved are short. Furthermore, since SDM

Manuscript received July 29, 2015; revised September 24, 2015; accepted October 9, 2015. Date of publication October 27, 2015; date of current version April 25, 2016. This work was supported by the Office of Naval Research Multidisciplinary Research Initiative, the US National Science Foundation (NSF), the NSF Center for Integrated Access Networks, the Defense Advanced Research Projects Agency, and the Cymer Corporation.

A. Grieco and Y. Fainman are with the Department of Electrical and Computer Engineering, University of California, San Diego CA 92093 USA (e-mail: agrieco@ucsd.edu; fainman@eng.ucsd.edu).

G. Porter is with the Department of Computer Science and Engineering, University of California, San Diego CA 92093 USA (e-mail: gmporter@cs.ucsd.edu).

Color versions of one or more of the figures in this paper are available online at http://ieeexplore.ieee.org.

Digital Object Identifier 10.1109/JSTQE.2015.2492361

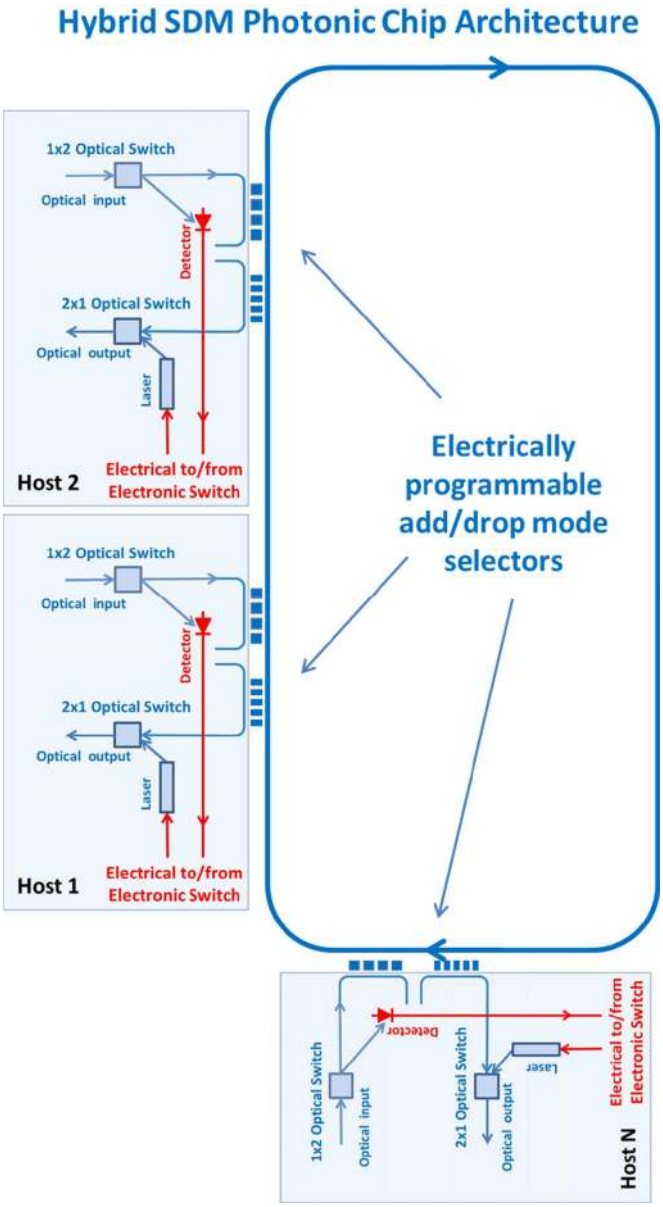

Fig. 1. Schematic of the proposed switch architecture. Conceptual illustration of the proposed switch architecture system showing the combined electronic packet switch and SDM circuit switch on a chip with a controller.

and WDM operate using separate degrees of freedom, combining such systems multiplies the available channel density for minimal overhead. The prospect of developing integrated SDM is tantalizing because it promises a substantial advantage in scalability and control as well as reduction in the cost and complexity of networking systems.

Selective mode excitation on an integrated photonic chip has been demonstrated in a number of ways, including the use of multimode interference couplers [23], asymmetric Y-couplers [24], photonic crystals [25], and an elaborate arrangement of ring resonators [18]. It is also possible using nonlinear optical effects [26]. Nonetheless, practical adoption of these technologies has been stymied by a number of drawbacks. These include issues such as large device footprints that result in low packing

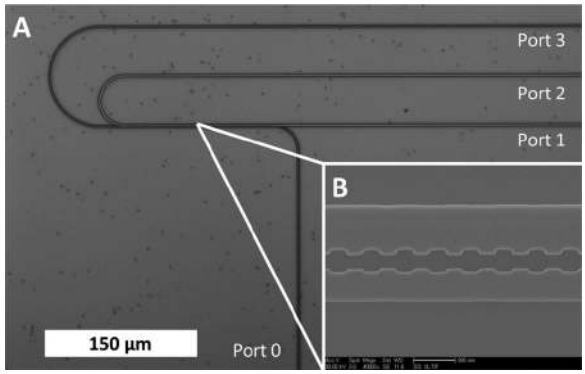

Fig. 2. Schematic of the periodically structured mode selective coupler. (A) Microscope image of the experimental device. Port 0 is the device input (e.g., from the jth Host in Fig. 1), Port 1 is the drop output (e.g., the multimode waveguide connecting N Hosts in Fig. 1), and Port 3 is the pass output. (B) Electron micrograph of the periodic waveguide perturbation. Note that the scale bar reads 500 nm.

density, a limited number of accessible high order modes, limited channel bandwidth, and a level of complexity that inhibits system design.

In this manuscript we introduce and demonstrate selective coupling between arbitrary spatial waveguide modes induced by a periodically nanostructured resonant waveguide, shown in Fig. 2(A) and (B). This is an extremely versatile design that possesses a number of distinct advantages in the context of SDM, namely: the coupler occupies a small area, resulting in a small device footprint and high packing density to support large OCS port count, the bandwidth of the device can be designed arbitrarily large or small, and may be controlled independently of the mode coupling, and there is no fundamental limit on the number of higher order modes that can be excited. It should be noted that each coupler can be reprogrammed to operate with a large number of different spatial modes, topologically enabling realization of crossbar switching.

II. Theory

The effect of periodically structuring a waveguide is best described using the paradigm of electromagnetic coupled-mode theory [27]–[30]. In this context the permittivity $\varepsilon(x,y,z)$ of the waveguide is represented as a Fourier series $\varepsilon(x,y,z) = \varepsilon_m(x,y) \cdot \exp(-i \cdot m \cdot 2\pi/\Lambda \cdot z)$, where m is an integer and Λ is the period of the perturbation. The full solution of Maxwell's equations is then written as a combination of the modes of the unperturbed z-invariant waveguide described by the 0th order term $\varepsilon_0(x,y)$ of the Fourier series. The effect of the periodic structuring is thus to transfer energy from one mode to another, although the transfer is generally not significant unless the difference between the wavenumbers of the interacting modes is approximately equal to $m \cdot 2\pi/L$ for some m. This is known as the longitudinal phase matching condition.

Each periodic structure in a waveguide typically only induces coupling between a single pair of modes. This is because the number of other propagating modes is limited, and their wavenumbers are not generally longitudinally phase matched by any grating order, allowing the coupling into these modes to

be neglected. Likewise, any energy that is coupled into radiating modes rapidly leaves the waveguide and may be accounted for as propagation loss. In the absence of loss, the differential equations that govern the interacting mode field amplitudes A_1 and A_2 are:

$$\begin{aligned}\frac{dA_1}{dz} &= -i\frac{\beta_1}{|\beta_1|}\kappa_1 \cdot A_2 \cdot \exp\left(i \cdot \Delta\beta \cdot z\right)\\ \frac{dA_2}{dz} &= -i\frac{\beta_2}{|\beta_2|}\kappa_2 \cdot A_2 \cdot \exp\left(-i \cdot \Delta\beta \cdot z\right).\\ \Delta\beta &= \beta_1 - \beta_2 - m\frac{2\pi}{\Lambda}\end{aligned} \tag{1}$$

The β coefficients indicate modal wavenumber. The coupling coefficients κ represent the strength of the interaction caused by the periodic structure, and are a function of the *m*th Fourier series component of the permittivity, and the extent to which it overlaps with the electric field vectors **E**(x,y) of the interacting modes:

$$\kappa_{1,2} = \frac{\omega}{2} \times \frac{\int_{-\infty}^{\infty}\int_{-\infty}^{\infty} \varepsilon_{\pm m}\left(x,y\right)\mathbf{E}_{2,1}\left(x,y\right)\cdot\mathbf{E}_{1,2}\left(x,y\right)^* dxdy}{\frac{v_{1,2}}{2}\int_{-\infty}^{\infty}\int_{-\infty}^{\infty}\varepsilon_0\left(x,y\right)\mathbf{E}_{1,2}\left(x,y\right)\cdot\mathbf{E}_{1,2}\left(x,y\right)^* dxdy}. \tag{2}$$

The ω and ν coefficients indicate the angular frequency and energy velocity of the optical field, respectively.

The exact solution of (1) depends on whether the interacting fields are co-propagating or counter-propagating. In the counter-propagating case, the solution for a structure of length *L* may be expressed in terms of a coefficient of reflection *r* and a coefficient of transmission *t*:

$$\begin{aligned} r &= \frac{A_2\left(0\right)}{A_1\left(0\right)} = \frac{-i\cdot\kappa_2\cdot L}{\frac{i\cdot\Delta\beta\cdot L}{2} + \frac{s\cdot L}{\tanh\left(s\cdot L\right)}}\\ t &= \frac{A_1\left(L\right)}{A_1\left(0\right)} = \frac{\frac{s\cdot L\cdot\exp\left(\frac{i\cdot\Delta\beta\cdot L}{2}\right)}{\sinh\left(s\cdot L\right)}}{\frac{i\cdot\Delta\beta\cdot L}{2} + \frac{s\cdot L}{\tanh\left(s\cdot L\right)}}\\ s &= \sqrt{\kappa_1\cdot\kappa_2 - \left(\frac{\Delta\beta}{2}\right)^2}. \end{aligned} \tag{3}$$

For a modal field incident on the periodic structure the coefficient of reflection indicates the fraction of field amplitude coupled into the counter-propagating mode. Likewise, the coefficient of transmission indicates the fraction of the incident modal field amplitude that exits the periodic structure.

A number of general observations may be drawn from equation (3). The coefficients of reflection and transmission have a spectral dependence. In the absence of loss, the points $\Delta\beta^2 = 4\cdot\kappa_1\cdot\kappa_2$ give $s = 0$ and are conventionally described as the edges of the reflection band (although the reflection is technically nonzero at these points). True reflection null points occur when $s\cdot L = n\cdot i\cdot p$ for integers $n \neq 0$, which causes the hyperbolic tangent to vanish. In contrast, the maximum reflection occurs at the center of the reflection band where $\Delta\beta = 0$. Since $\kappa_1, \kappa_2, \Delta b$, and L are engineered quantities it is possible to exert control over every aspect of the reflection band.

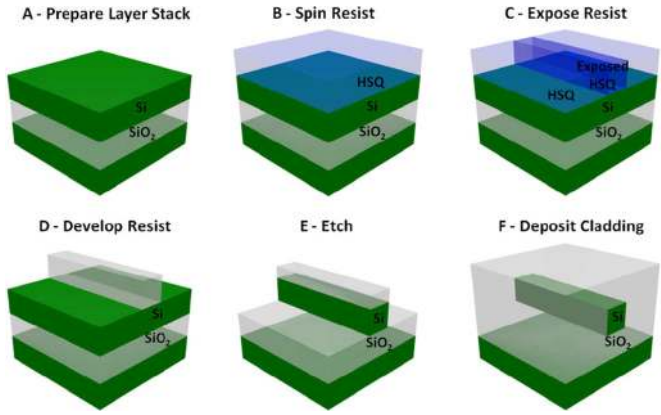

Fig. 3. Illustration of the fabrication process.

In the appropriate limits equation (3) describes a broad range of phenomena, including Bragg reflection [11], evanescent coupling [12], [13], [31], and dispersion engineering [32]. Notably, conventional applications have been limited to coupling within or between single mode waveguides. However, from close inspection of (1) through (3) it is clear this need not be the case. Formally, it is possible to couple any two modes that overlap spatially with the dielectric perturbation. In general guided modes have exponentially decaying tails that lie outside of the waveguide core, so this mechanism includes coupling modes within a single multimode waveguide, and coupling multiple modes of adjacent multimode waveguides. The opportunities afforded by coupling in multimode waveguides form the basis for the proposed SDM device.

III. Experimental Demonstration

A. Fabrication and Characterization

The fabrication process is illustrated in Fig. 3. The waveguides are created from a SOI substrate with a 220 nm silicon top layer in [100] orientation, and a 3 μm buried oxide layer composed of thermally grown silicon dioxide. The substrate is then spin coated with a layer of hydrogen silsesquioxane electron beam resist, and the wafers are patterned by electron beam lithography. The exposed resist is developed in a tetramethylammonium hydroxide solution. The waveguides are then formed by an inductively coupled plasma reactive-ion etch. The sample is then cladded with a layer of plasma-enhanced chemical vapor deposition silicon dioxide, and the waveguides are exposed by dicing. It is not necessary to remove the resist following etching because it is converted to silicon dioxide during the development process.

The nominal dimensions of the experimental device are 400 by 220 nm for the single-mode waveguide, and 600 by 220 nm for the multi-mode waveguide. The perturbation is created by modulating the waveguide widths by 10% in a square wave pattern with a period of 392 nm and a total length of 383 periods ($\sim$150 microns). The input port of the device is tapered to a width of 200 nm to facilitate coupling from the lensed tapered fiber. Using a refractive index of 3.48 for silicon and 1.46 for silicon dioxide and a wavelength of 1490 nm the calculated effective

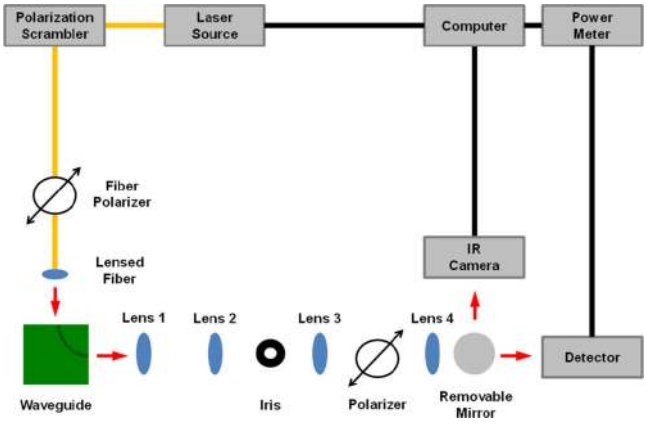

Fig. 4. Illustration of the experimental setup.

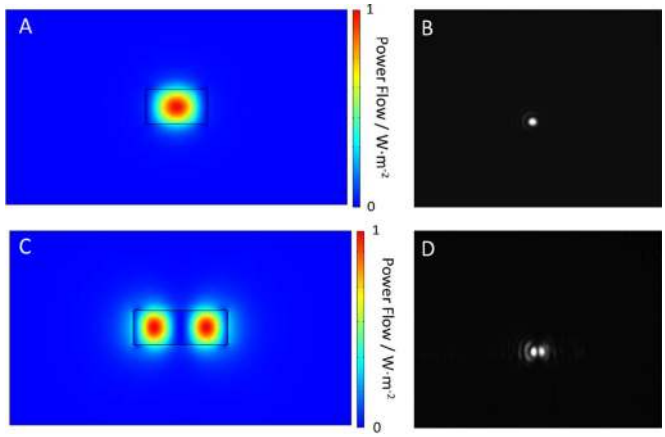

Fig. 5. Theoretical and experimental mode profiles of the SDM. (A) Theoretical mode profile (unnormalized) of output Port 3 at 1475 nm wavelength showing the transmission of the single mode input waveguide outside of the operating band of the SDM coupler. (B) Experimental mode profile of output Port 3 at 1475 nm wavelength. (C) Theoretical mode profile (unnormalized) of output Port 1 at 1490 nm wavelength showing the second order mode excited by the SDM at its resonant wavelength. (D) Experimental mode profile of output Port 1 at 1490 nm wavelength.

refractive index of the first order mode is 2.25, and the second order mode is 1.73. For these dimensions the predicted band center is 1560 nm, which is within 5% of the experimental value. This discrepancy is a consequence of the variation inherent in the fabrication process, and the approximations inherent in formulating the coupled-mode interaction through perturbation theory. Generally speaking, the impact of fabrication variation may be reduced by increasing the scale of the device, and the impact of the theoretical approximations may be reduced by making the dielectric modulation more perturbative.

The characterization of the multiplexer was performed using the experimental setup illustrated in Fig. 4. The tunable laser source (Agilent model 81980A) is fiber coupled to a polarization scrambler, a fiber polarizer, and a lensed tapered fiber. The input of the waveguide is excited by the lensed tapered fiber, and a microscope objective (lens 1 in Fig. 4) is used to collect the output. The light is then imaged on a detector by two sequential 4F systems (formed by lenses 1–2 and 3–4 in Fig. 4). The iris in the first focal plane serves to eliminate stray light from around the waveguide output, and a polarizer in the second Fourier plane is used to reject any unwanted polarization component that might arise from imperfect alignment of the input lensed tapered fiber. A removable mirror in the optical path can be used to direct the waveguide output to an infrared camera (ICI model Alpha NIR) for imaging, or a detector (Newport model 918D-IG-OD3) for power characterization. Measurements are automated by a computer which coordinates the laser source and power meter (Newport model 2936-R). The uncertainty in each power measurement is $\pm 1\%$, and the variation of source output power versus wavelength is less than $\pm 6\%$. The nominal laser output for the experimental measurement was 10 dBm, however coupling to the waveguide was suboptimal because the output of the lensed tapered fiber was defocused to minimize impact of mechanical drift over the course of the measurement.

IV. Results and Discussion

The experimental device in Fig. 2 is an SDM coupler that transfers energy from the fundamental TE-mode of the single mode input waveguide at Port 0 (from e.g., the jth host in Fig. 1) to the counter-propagating second order TE-mode of the multimode output waveguide at Port 1 (forming a connection of the jth host to the multimode waveguide) about a resonance wavelength. Energy not transferred by the coupler remains in the single mode waveguide and ultimately exits the device at Port 3, used here to help detect how much energy from Port 0 has been converted to the multimode waveguide at Port 1 via the multimode converter. To verify that the coupling occurred between the desired modes the intensity profile at the device output ports was characterized using an infrared camera. The results are presented in Fig. 5 along with the theoretically predicted intensity profiles. Away from the resonance wavelength of the coupler, the optical energy remains in the single mode waveguide, which is in accordance with the theoretical and experimental profiles of the fundamental mode in Fig. 5(A) and (B). The excellent agreement of the theoretical and experimental second order mode profiles in Fig. 5(C) and (D) at the resonance wavelength of the coupler makes it clear that the selective excitation of higher order modes in the multimode waveguide was successful. The distinct null in the center of the experimental second order mode profile is a strong indication that no incidental coupling occurred into the symmetric lower order modes. The transmission spectra of the device output ports are presented in Fig. 6. The mode coupling occurs in a 10 nm broad wavelength band centered at $\sim$1490 nm, with a maximum extinction of $\sim$22 dB. Note that such a design can tolerate the wavelength fluctuations that may occur in low cost transceivers from numerous hosts connected to our SDM switch, leading to the robustness of our approach. The total loss of the experimental coupler is $\sim$3 dB. This loss is a consequence of mode mismatch between the unperturbed waveguide and the periodically structured device. It has been demonstrated experimentally that by tapering the transition to the periodic perturbation that this source of loss can be eliminated [33]. Such tapers would not appreciably contribute to the length of the device. Otherwise, the loss of the structure will approach that of the unperturbed waveguide, which is typically

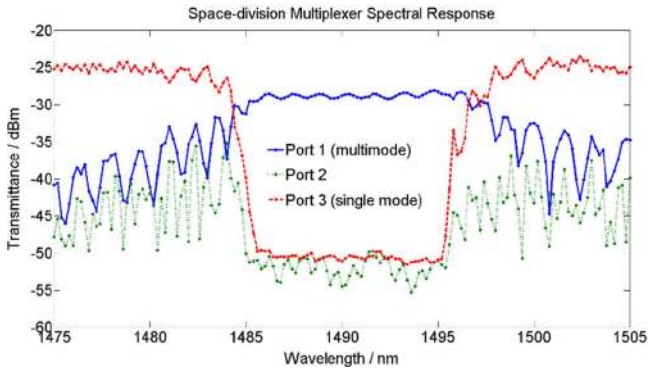

Fig. 6. Experimental transmission spectra of the periodically structured mode coupler. The port listing corresponds to Fig. 2. Light enters the single mode input waveguide at Port 0. The multimode waveguide is excited at the coupler resonance and the light exits at Port 1. Off resonance the light remains in the single mode waveguide and exits at port 3.

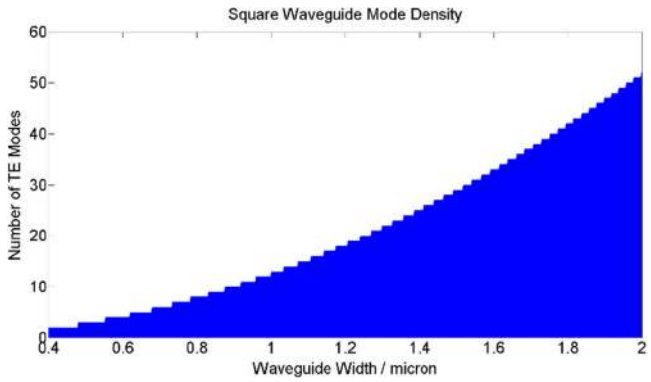

Fig. 7. Mode density of a square silicon-on-insulator waveguide.

around ∼5 dB/cm [27], indicating that for a total device length of up to 1 mm the net losses are negligible.

A primary figure of merit of a multiplexing scheme is the number of channels it can support. In this case, the fundamental channel limit is the maximum number of modes supported by the multimode waveguide. The number of TE (or equivalently TM) modes supported by a strip waveguide with square cross section may be expressed approximately as [34]:

$$M \approx \frac{\pi}{4}\left(\frac{2\cdot d}{\lambda_0}\right)^2 \left(n_{\text{core}}^2 - n_{\text{cladding}}^2\right). \tag{4}$$

In this expression M represents the mode number (when rounded down), d is the waveguide width, λ_0 is the free-space wavelength, and n is the waveguide refractive index. The TE (or equivalently TM) mode density in a typical SOI waveguide is plotted in Fig. 7 in accordance with equation (4). The mode density is calculated for a free-space wavelength of 1550 nm, a core refractive index of 3.48 (corresponding to silicon) and a cladding refractive index of 1.46 (corresponding to silicon dioxide). A 2 micron wide square waveguide with these parameters supports 50 TE modes and 50 TM modes. It is clear that SDM channel density compares favorably with WDM even when considered as a standalone technology.

In the context of scalability, it is much more efficient to avoid optical-electronic conversion and perform switching optically whenever possible. Existing WDM optical interconnect architectures rely on thermal switching mechanisms [35], [36]. For a nanosecond SDM interconnect architecture there are a limited number of physical mechanisms available that are capable of switching at the required speed, carrier injection being the most proven technology [37], [38]. Devices based on these effects operate using the dependence of waveguide refractive index on the temperature or carrier density. The refractive index of the waveguide alters the effective index of the guided modes, and thereby the longitudinal phase matching condition of the SDM coupler. This may be used to tune the coupler between modes, or spoil the coupling, since the phase matching condition is very stringent. Assuming that the tuning response of each waveguide is the same, for a switching effective index change of Δn_{eff} the maximum channel bandwidth is $\Delta\lambda_{\text{BW}} = 4\cdot\Lambda\cdot m\cdot\Delta n_{\text{eff}}$ for grating order m.

Finally, it should be noted that for integrated waveguides the dominant source of loss is scattering produced by roughness in the waveguide sidewalls [39]. Consequently, increasing the waveguide dimensions reduces loss because less of the mode overlaps with the waveguide sidewalls. For the same the loss of higher order modes tends to be less than that of lower order modes. The caveat is that higher order modes tend to be less confined and therefore more susceptible to bending loss. In practice this situation may be avoided by not bending the multimode waveguide.

V. Conclusion

The SDM coupler demonstrated here has significant implications for optical networking. The device mitigates the shortcomings of alternative SDM schemes by possessing advantages in terms of packing density, control of operating bandwidth, tunability to operate with numerous orthogonal spatial modes, and support of large number of switching ports. Furthermore, the periodic structure that forms the backbone of the device can be used to perform additional signal processing functions with minimal impact on the device footprint [32]. Integrated SDM has the potential to reduce the cost and complexity of networking systems, either by improving scalability through the augmentation of existing WDM schemes, or as a standalone technology by eliminating the need for costly WDM components.

Acknowledgment

The authors would like to thank the Nano3 staff at UCSD for support during sample fabrication. They would also like to thank Claudette Hennessey for logistical support.

References

[1] H. Bazzaz *et al.*, "Switching the optical divide: Fundamental challenges for hybrid electrical/optical datacenter networks," presented at the ACM Symp. Cloud Computing, Cascais, Portugal, 2011.

[2] K. Chen *et al.*, "OSA: An optical switching architecture for data center networks with unprecedented flexibility," presented at the 9th USENIX Conf. Networked Systems Design Implementation, San Jose, CA, USA, 2012.

[3] N. Farrington *et al.*, "Helios: A hybrid electrical/optical switch architecture for modular data centers," in *Proc. ACM SIGCOMM Conf.*, New Delhi, India, 2010, pp. 339–350.

[4] N. Farrington, Y. Fainman, H. Liu, G. Papen, and A. Vahdat, "Hardware requirements for optical circuit switched data center networks," presented at the Optical Fiber Communication Conf./Nat. Fiber Optic Engineers Conf., Los Angeles, CA, USA, 2011.

[5] G. Wang *et al.*, "c-Through: Part-time optics in data centers," in *Proc. SIGCOMM Conf.*, New Delhi, India, 2010, pp. 327–338.

[6] N. Farrington, G. Porter, Y. Fainman, G. Papen, and A. Vahdat, "Hunting mice with microsecond circuit switches," in *Proc. 11th ACM Workshop Hot Topics Netw.*, Redmond, WA, USA, 2012, pp. 115–120.

[7] N. Farrington *et al.*, "A demonstration of ultra-low-latency datacenter optical circuit switching," presented at the ACM SIGCOMM Conf., Helsinki, Finland, 2012.

[8] G. Porter *et al.*, "Integrating microsecond circuit switching into the data center," in *Proc. ACM SIGCOMM Conf. SIGCOMM*, Hong Kong, China, 2013, pp. 447–458.

[9] Y. Fainman and G. Porter, "Directing data center traffic," *Science*, vol. 342, pp. 202–203, 2013.

[10] H. Liu *et al.*, "Circuit switching under the radar with reactor," in *Proc. 11th ACM/USENIX Symp. Netw. Syst. Design Implementation*, Seattle, WA, USA, 2014, pp. 1–15.

[11] H.-C. Kim, K. Ikeda, and Y. Fainman, "Tunable transmission resonant filter and modulator with vertical gratings," *J. Lightw. Technol.*, vol. 25, no. 5, pp. 1147–1151, May 2007.

[12] K. Ikeda, M. Nezhad, and Y. Fainman, "Wavelength selective coupler with vertical gratings on silicon chip," *Appl. Phys. Lett.*, vol. 92, art. no. 201111, 2008.

[13] D. T. H. Tan *et al.*, "Wide bandwidth, low loss 1 by 4 wavelength division multiplexer on silicon for optical interconnects," *Opt. Exp.*, vol. 19, pp. 2401–2409, 2011.

[14] O. Bondarenko *et al.*, "Wafer bonded distributed feedback laser with sidewall modulated bragg gratings," *Appl. Phys. Lett.*, vol. 103, art. no. 043105, 2013.

[15] O. Bondarenko *et al.*, "Wafer bonded subwavelength metallo-dielectric laser," *IEEE Photon. J.*, vol. 3, no. 3, pp. 608–616, Jun. 2011.

[16] M. P. Nezhad *et al.*, "Room-temperature subwavelength metallo-dielectric lasers," *Nature Photon.*, vol. 4, pp. 395–399, 2010.

[17] K.-P. Ho and J. M. Kahn, "Mode coupling and its impact on spatially multiplexed systems," in *Proc. Opt. Fiber Telecommun. VI*, 2013, pp. 491–568.

[18] L.-W. Luo *et al.*, "WDM-compatible mode-division multiplexing on a silicon chip," *Nature Commun.*, vol. 5, art. no. 3069, 2014.

[19] S. O. Arik, J. M. Kahn, and K.-P. Ho, "MIMO signal processing for mode-division multiplexing: An overview of channel models and signal processing architectures," *Signal Process. Mag.*, vol. 31, pp. 25–34, 2014.

[20] S. Berdagué and P. Facq, "Mode division multiplexing in optical fibers," *Appl. Opt.*, vol. 21, pp. 1950–1955, 1982.

[21] H. R. Stuart, "Dispersive multiplexing in multimode optical fiber," *Science*, vol. 289, pp. 281–283, 2000.

[22] R. Rokitski and Y. Fainman, "Propagation of ultrashort pulses in multimode fiber in space and time," *Opt. Exp.*, vol. 11, pp. 1497–1502, 2003.

[23] L. B. Soldano and E. C. M. Pennings, "Optical multi-mode interference devices based on self-imaging: Principles and applications," *J. Lightw. Technol.*, vol. 13, no. 4, pp. 615–627, Apr. 1995.

[24] Y. Huang, G. Xu, and S.-T. Ho, "An ultracompact optical mode order converter," *Photon. Technol. Lett.*, vol. 18, pp. 2281–2283, 2006.

[25] V. Liu, D. A. B. Miller, and S. Fan, "Ultra-compact photonic crystal waveguide spatial mode converter and its connection to the optical diode effect," *Opt. Exp.*, vol. 20, pp. 28388–28397, 2012.

[26] A. Hasegawa and T. Nyu, "Eigenvalue communication," *J. Lightw. Technol.*, vol. 11, no. 3, pp. 395–399, Mar. 1993.

[27] A. Grieco, B. Slutsky, and F. Yeshaiahu, "Characterization of waveguide loss using distributed Bragg reflectors," *Appl. Phys. B*, vol. 114, pp. 467–474, 2014.

[28] A. Yariv and P. Yeh, *Optical Waves in Crystals: Propagation and Control of Laser Radiation*. Hoboken, NJ, USA: Wiley, 2003.

[29] H. Kogelnik, "2. Theory of dielectric waveguides," in *Integrated Optics (Topics in Applied Physics)*. Berlin, Germany: Springer-Verlag, 1975, pp. 13–81.

[30] D. J. Richardson, J. M. Fini, and L. E. Nelson, "Space-division multiplexing in optical fibres," *Nature Photon.*, vol. 7, pp. 354–362, 2013.

[31] D. T. H. Tan, K. Ikeda, and Y. Fainman, "Cladding-modulated Bragg gratings in silicon waveguides," *Opt. Lett.*, vol. 34, pp. 1357–1359, 2009.

[32] D. T. H. Tan, P. C. Sun, and F. Yeshaiahu, "Monolithic nonlinear pulse compressor on a silicon chip," *Nature Commun.*, vol. 1, art. no. 116, 2010.

[33] A. Grieco and Y. Fainman, "Characterization of distributed Bragg reflectors," *J. Quantum Electron.*, vol. 50, pp. 453–457, 2014.

[34] B. A. Saleh and M. C. Teich, *Fundamentals of Photonics*. Hoboken, NJ, USA: Wiley, 1991.

[35] S. Homampour, M. P. Bulk, P. E. Jessop, and A. P. Knights, "Thermal tuning of planar Bragg gratings in silicon-on-insulator rib waveguides," *Phys. Status Solidi C*, vol. 6, pp. S240–S243, 2009.

[36] X. Wang, J. A. Martinez, and M. S. Nawrocka, "Compact thermally tunable silicon wavelength switch: Modeling and characterization," *Photon. Technol. Lett.*, vol. 20, pp. 936–938, 2008.

[37] R. A. Soref and B. A. Bennett, "Electrooptical effects in silicon," *IEEE J. Quantum Electron.*, vol. QE-23, no. 1, pp. 123–129, Jan. 1987.

[38] C. Li, L. Zhou, and A. W. Poon, "Silicon microring carrier-injection-based modulators/switches with tunable extinction ratios and OR-logic switching by using waveguide cross-coupling," *Opt. Exp.*, vol. 15, pp. 5069–5076, 2007.

[39] F. Grillot, L. Vivien, S. Laval, D. Pascal, and E. Cassan, "Size influence on the propagation loss induced by sidewall roughness in ultrasmall SOI waveguides," *Photon. Technol. Lett.*, vol. 16, pp. 1661–1663, 2004.

Andrew Grieco received the B.S. degree both in physics and earth science (with geology option) from the New Mexico Institute of Mining and Technology, Socorro, NM, USA, in 2007, the M.S. degree in electrical engineering (with photonics option) from the University of California, San Diego, CA, USA, in 2010, and the Ph.D. degree in electrical engineering (with photonics option) from the University of California, San Diego, in 2014.

From 2007 to 2008, he was a Post-Baccalaureate Student Researcher with the Shock and Detonation Physics Group, Los Alamos National Laboratory. Since 2008, he has been a Researcher with the Department of Electrical Engineering, University of California, San Diego. His research interests include nonlinear optics and integrated photonics.

George Porter received the B.S. degree in computer science from the University of Texas at Austin, Austin, TX, USA, in 2001, the M.S. degree in computer science from the University of California, Berkeley, CA, USA, in 2003, and the Ph.D. degree in computer science from the University of California, Berkeley, in 2008.

He is the Associate Director of the Center for Networked Systems, and an Assistant Professor with the Department of Computer Science and Engineering, University of California, San Diego, CA, USA.

Yeshaiahu Fainman is a Cymer Professor of Advanced Optical Technologies and Distinguished Professor of electrical and computer engineering, University of California, San Diego (UCSD), San Diego, CA, USA. He is directing research of the Ultrafast and Nanoscale Optics group at UCSD and made significant contributions to near field optical phenomena, inhomogeneous and meta-materials, nanophotonics and plasmonics, and nonconventional imaging. The research applications target information technologies and biomedical sensing. His current research interests include near field optical science and technology. He contributed more than 220 manuscripts in peer review journals and more than 350 conference presentations and conference proceedings. He is a Fellow of the Optical Society of America, and Fellow of the Society of Photo-Optical Instrumentation Engineers. He received the Miriam and Aharon Gutvirt Prize, Lady Davis Fellowship, Brown Award, Gabor Award, and Emet Leith Medal.